Density Tapering of Linear Arrays Radiating Pencil Beams: A New Extremely Fast Gaussian Approach

Giulia Buttazzoni and Roberto Vescovo

***Abstract*— In this communication, a very simple and extremely fast algorithm is proposed for the pencil beam synthesis of linear sparse arrays having uniform distribution of the excitations. The key idea is that of selecting, as a desired pattern, a Gaussian function having small standard deviation, so as to obtain a narrow beam. This immediately provides the excitation density of the corresponding continuous array of infinite length. Starting from this result and considering a linear array of length L with N elements having equal excitations, an extremely fast and accurate algorithm based on a density tapering approach is proposed that yields suitable positions of the elements, in such a way as to provide an array factor that well approximates the desired pattern. Numerical examples are presented to show the effectiveness of the developed procedure, also when compared with state-of-the-art algorithms. The proposed approach does not consider the mutual coupling between the array elements, but it is numerically shown that this effect produces quite acceptable degradation on the synthesized patterns. Finally, it is shown that also problems involving thousands of elements can be solved in a very accurate way in few milliseconds.**

***Index Terms*— Density tapering, Gaussian distribution, geometrical synthesis, pencil beams, sparse antenna arrays.**

I. Introduction

From the very beginning of the antenna history, the idea has arisen of improving the radiation characteristics of a single radiator through the use of a collection of identical elements, suitably located and suitably fed. Soon, the theory of antenna arrays has gained attention thanks to the increased awareness in the great advantages they can provide [1]. A great number of synthesis techniques have been devised for arrays of assigned geometry, based on both deterministic and stochastic approaches [1]–[5]. Since the sixties of last century, attention has been devoted to the problem of calculating the optimal positions of the array elements [6]–[8]. It is clear, in fact, that the possibility of modifying the element positions (geometrical synthesis [9]) offers more degrees of freedom compared with the case where the array geometry is assigned [2]. Thus, when synthesizing also the element positions along with their excitations, fewer elements are needed to achieve the same performances, or better performances can be achieved with the same number of elements [10]. Of course, in applications that require a uniform distribution of the excitations, the only degrees of freedom available to the designer are those concerning the element positions. However, this may be sufficient to produce quite satisfactory performances, and allows a simpler feeding network. For example, nonuniformly spaced linear arrays with uniform distribution can reduce the maximum sidelobe level even much below the −13.46 dB threshold that characterizes uniformly spaced uniformly fed linear arrays. Despite its remote origin, the geometrical synthesis of linear arrays with uniform distribution of the excitations is still a hot topic in the antenna community, and many synthesis algorithms have been developed in the last years, based either on stochastic procedures [11]–[14] or on deterministic approaches [15]–[17].

In this communication, the problem of synthesizing a pencil beam with a linear sparse array of uniformly fed elements is addressed. To this aim, the so-called *density tapering* technique [15] is used in conjunction with an original and clever choice of the function representing the desired pencil beam, which is selected as a Gaussian function whose standard deviation controls the beamwidth. It is precisely thanks to this choice that convenient element positions are determined in a very easy closed form, and the synthesis problem is solved in a very easy, fast, and accurate way.

This communication is organized as follows. In Section II, the formulation of the problem is presented, and the synthesis algorithm is described in detail. Section III shows some numerical examples, which validate the proposed approach also in comparison with state-of-the-art algorithms. Finally, the conclusions are summarized in Section IV.

II. Formulation of the Problem

Given a Cartesian system $O(x, y, z)$, consider a linear array of N elements located at the positions $z_1, \ldots, z_N$ on the z-axis. The array factor is given by

$$F(\mathbf{a}; u) = \sum_{n=1}^{N} a_n \exp(juz_n) \tag{1}$$

where $\mathbf{a} = [a_1, \ldots, a_N]^T$ is the column vector of the complex excitations, and $u = k \sin \vartheta$ where $k = 2\pi/\lambda$, with λ the wavelength and ϑ the angle from broadside (i.e., the elevation angle). As usual, in (1), the variable u takes all real values. However, since $-\pi/2 \leq \vartheta \leq \pi/2$, the values of u in the interval $-k \leq u \leq k$ specify the visible pattern, while the values $|u| > k$ specify the invisible pattern.

The aim of this communication is that of solving the following problem: given a linear array of assigned length L_a and consisting of a given number N of elements having uniform excitation, find the element positions in such a way that the corresponding array factor [see (1), with $a_n = 1, n = 1, \ldots, N$] be a pencil beam having a given width. The proposed approach moves from the well-known possibility of extending (1) to represent the radiation pattern of a linear antenna of length L, characterized by an excitation density $a(z)$, ($|z| \leq L/2$), obtaining

$$F(a; u) = \int_{-L/2}^{L/2} a(z) \exp(juz) dz. \tag{2}$$

The proposed solving procedure starts introducing a suitable desired pattern $F_d(u)$, representing a pencil beam with the prescribed

Manuscript received October 20, 2016; revised July 6, 2017; accepted October 17, 2017. Date of publication October 23, 2017; date of current version November 30, 2017. This work was supported by the Italian Ministry of University and Research under Project FRA 2015. *(Corresponding author: Giulia Buttazzoni.)*

The authors are with the Department of Engineering and Architecture, University of Trieste, 34127 Trieste, Italy (e-mail: gbuttazzoni@units.it; vescovo@units.it).

Color versions of one or more of the figures in this communication are available online at http://ieeexplore.ieee.org.

width. Then, the procedure develops in the following three steps: 1) an excitation density $a(z)$ is determined for $-\infty<z<+\infty$ [i.e., $L = +\infty$ in (2)], which exactly produces the pencil beam $F_d(u)$ [i.e., $F(a; u) = F_d(u)$]; 2) from the assigned array length L_a, a finite "equivalent length" $L(>L_a)$ to be used in (2) is determined for the "continuous" array; and 3) the density tapering technique [15] is applied to $a(z)$ to determine the optimal positions z_n of the array elements. Due to our Gaussian choice, the positions z_n resulted to belong to the assigned interval $[-L_a/2, L_a/2]$, as required, and are calculated in closed form. This allows a dramatic reduction of the computational burden. This innovative Gaussian approach is described in detail in Sections II-A and II-B, and is summarized in Section II-C.

A. Gaussian Approach

The key idea of this communication is that of using, as the desired pattern $F_d(u)$, a Gaussian function. The reasons are twofold: 1) by selecting a sufficiently small standard deviation, it represents a pencil beam of arbitrarily small width and 2) the Fourier transform of a Gaussian function is another Gaussian function (up to a multiplicative constant), having reciprocal standard deviation. This allows to calculate immediately, and in closed form, the excitation density in an array of infinite length that produces the required pencil beam. In the sequel, it is shown that, thanks to this Gaussian choice, the proposed synthesis procedure yields the optimal element positions in closed form, and in an extremely fast, simple, and accurate way.

A Gaussian function of mean value 0 and mean-square deviation σ is defined as $f(u) = (1/\sigma\sqrt{2\pi})\exp(-u^2/2\sigma^2)$. This function is here normalized and used to represent the desired array factor as

$$F_d(u) = \exp\left(-\frac{u^2}{2\sigma^2}\right). \tag{3}$$

The mean-square deviation σ is used to control the "width" of $F_d(u)$, which is small for low values of σ. Precisely, imposing that the b-dB beamwidth be $\mathrm{BW}_{\mathrm{deg}}$ (degrees), using (3), σ must be

$$\sigma = k\sqrt{\frac{10}{b\ln 10}}\sin\left(\frac{\pi\,\mathrm{BW}_{\mathrm{deg}}}{360}\right). \tag{4}$$

Equation (4) yields σ, and therefore specifies the desired pattern in (3). Now, the excitation density $a(z)$ defined for $-\infty<z<+\infty$ that (exactly) produces $F_d(u)$ can be immediately calculated. In fact, $2\pi a(z)$ is the Fourier transform of $F_d(u)$, that is, $2\pi a(z) = \int_{-\infty}^{\infty} F_d(u)\exp(-jzu)du$ [3], and the Fourier transform of a Gaussian function is a Gaussian function with reciprocal standard deviation, up to a multiplicative constant. Precisely, it results

$$a(z) = \frac{\sigma}{\sqrt{2\pi}}\exp\left(-\frac{\sigma^2 z^2}{2}\right). \tag{5}$$

Therefore, substituting (5) into (2) with $L = +\infty$ yields exactly $F_d(u)$, that is

$$F_d(u) = \int_{-\infty}^{+\infty}\frac{\sigma}{\sqrt{2\pi}}\exp\left(-\frac{\sigma^2 z^2}{2}\right)\exp(juz)dz. \tag{6}$$

Instead, assuming a finite length L, (2) yields the pattern

$$F_L(u) = \int_{-L/2}^{L/2}\frac{\sigma}{\sqrt{2\pi}}\exp\left(-\frac{\sigma^2 z^2}{2}\right)\exp(juz)dz \tag{7}$$

which approximates $F_d(u)$. On the other hand, the aim of this communication is that of finding the optimal positions of a finite number N of elements belonging to an array of assigned length L_a, rather than an excitation density defined in a "continuous" array of length L. However, the proposed algorithm determines the N optimal positions $z_1, \ldots, z_N$ as functions of L within the interval $[-L/2, L/2]$ (see below). Thus, the length L is selected in such a way that these positions belong to the interval $[-L_a/2, L_a/2]$. More precisely, L is selected in such a way that $z_1 = -L_a/2$ and $z_N = L_a/2$, and thus $z_N - z_1 = L_a < L$. In the Appendix, two relations [(16) and (19)] are obtained between L and L_a, in correspondence of two different criteria of choice of the element positions. Such relations allow to easily calculate the appropriate value of L corresponding to an assigned value of L_a in a very fast and accurate way. Once L is calculated, the optimal positions z_n are determined by the procedure described in the next section.

B. Density Tapering Approach and Gaussian Distribution

Given a suitable finite length L for the excitation density in (5), (7) provides an approximation of the desired pattern $F_d(u)$. In order to synthesize an antenna array of N elements, the interval $-L/2 \le z \le L/2$ is divided into N subintervals $I_n = [s_{n-1}, s_n]$, $n = 1, \ldots, N$, where $s_0 = -L/2$ and $s_N = L/2$. The pattern $F_L(u)$ in (7) can be expressed as follows:

$$F_L(u) = \sum_{n=1}^{N}\int_{s_{n-1}}^{s_n} a(z)\exp(juz)dz \tag{8}$$

where $a(z)$ is given by (5). In order to approximate (8) with the array factor in (1), the nth integral in (8) is approximated by the term $a_n\exp(juz_n)$ in (1). To do so, the variables a_n and z_n need to be suitably selected. Here, the following choices have been adopted:

$$a_n = \int_{s_{n-1}}^{s_n} a(z)dz \tag{9a}$$

$$z_n = \frac{1}{a_n}\int_{s_{n-1}}^{s_n} a(z)z\,dz. \tag{9b}$$

The choice (9b) for the positions z_n is that suggested in [15] for uniform distribution of the excitations. Note that, with this choice, z_n is the abscissa of the barycenter of the area located between the diagram of $a(z)$ and the interval I_n. The choice in (9b) can be replaced by the simpler one

$$z_n = \frac{s_{n-1} + s_n}{2} \tag{9c}$$

which yields the middle point z_n of I_n. The numerical results in Section III have been obtained with the choice in (9b). Using the choice in (9c), the results were essentially the same, so they are not shown.

In order to obtain a sparse array with uniform distribution of the excitations, we here adopt the so-called *density taper* (or *space taper*) approach [7], [15]. Precisely, the points s_n in (9a) are calculated in such a way that all of the excitations a_n be equal to the area $A = \int_{-L/2}^{L/2} a(z)dz$ divided by N, that is, using (5)

$$a_n = a_0 = \frac{1}{N}\int_{-L/2}^{L/2} a(z)dz = \frac{1}{N}\,\mathrm{erf}\left[\frac{\sigma L}{2\sqrt{2}}\right] \tag{10}$$

where $\mathrm{erf}(x) = (2/\sqrt{\pi})\int_0^x \exp(-t^2)dt$ is the error function. So, the area of the region between the diagram of $a(z)$ and the interval I_n must be the same for all intervals. This area, equal to a_0, is assumed as the common value of all excitations.

With this approach, recalling (5) and (10), the points s_n in (9a) must satisfy the condition

$$\frac{\sigma}{\sqrt{2\pi}}\int_{-L/2}^{s_n}\exp\left(-\frac{\sigma^2 z^2}{2}\right)dz = \frac{1}{2}\left[\mathrm{erf}\left(\frac{\sigma s_n}{\sqrt{2}}\right) + \mathrm{erf}\left(\frac{\sigma L}{2\sqrt{2}}\right)\right] = na_0. \tag{11}$$

Solving (11) for s_n yields, recalling (10)

$$s_n = \frac{\sqrt{2}}{\sigma}\,\mathrm{erf}^{-1}\left[\left(\frac{2n}{N}-1\right)\mathrm{erf}\left(\frac{\sigma L}{2\sqrt{2}}\right)\right] \tag{12}$$

where erf^{-1} is the inverse of the error function. Adopting the choice (9b) for the positions z_n of the N array elements and using (5), after some manipulations, one obtains

$$z_n = \frac{N}{\sigma\sqrt{2\pi}\,\mathrm{erf}\left[\frac{\sigma L}{2\sqrt{2}}\right]}\left[\exp\left(-\frac{\sigma^2 s_{n-1}^2}{2}\right)-\exp\left(-\frac{\sigma^2 s_n^2}{2}\right)\right]. \tag{13}$$

So, once the points s_n have been calculated by (12), the required positions z_n can be found by (13) or, as stated above, by using the simpler choice (9c), and the array factor can be calculated by (1). Note that the quantities s_n can be determined in closed form by (12) thanks to the Gaussian choice in (3). With a different choice, the computation of s_n would require a much more complicated procedure (see [16] for example), and therefore a much higher CPU time. It is also to be noted that, due to the adoption of a finite length L for the "continuous" array, and to the successive discretization of the problem, the resulting beamwidth is expected to be larger than that of $F_d(u)$, which is controlled by the mean-square deviation σ. This beam widening is negligible for large arrays (see the first example in Section III), but has to be taken into account for smaller arrays (second to fifth examples in Section III). Thus, in the latter cases, the choice of σ by (4) is critical. However, it has been heuristically found that introducing in (4) a 3 dB beamwidth $\mathrm{BW}_{\mathrm{deg}}$ equal to the desired one divided by 2 produces a pencil beam with the desired beamwidth. That is, in (4), it can be set $\mathrm{BW}_{\mathrm{deg}} = \mathrm{BW}_{\mathrm{deg}}^{\mathrm{desired}}/2$ with $b = 3$. This simple rule of thumb has been adopted for Examples 2–5 and has provided the patterns in Figs. 3–6.

C. Algorithm

To conclude, the problem and the synthesis algorithm can be summarized as follows. Given the b dB beamwidth $\mathrm{BW}_{\mathrm{deg}}^{\mathrm{desired}}$ of a desired pencil beam, the number N of the array elements, and the assigned length L_a of the array, the developed synthesis procedure consists in evaluating σ with (4), finding the length L by solving (16) or (19) in the Appendix, calculating the points s_n with (12), and calculating the positions z_n, $n = 1, \ldots, N$, with (13) or (9c).

The next section presents five numerical examples which prove the validity of the proposed algorithm.

III. Numerical Examples

In this section, some numerical examples are presented, to validate the proposed synthesis algorithm. First, a sparse array composed by a great number of elements is synthesized, which radiates a very narrow pencil beam. This represents the setup for which the proposed approach has been thought. Arrays involving a great number of elements (of the order of hundreds) can have satellite applications, and are expected to be used in future 5G communication networks. Then, after an accurate analysis of the previous literature concerning the methods of pencil-beam synthesis of sparse arrays with uniform amplitude distribution, the most significant examples have been selected. For each example, the algorithm presented in Section II has been applied setting the parameters b and $\mathrm{BW}_{\mathrm{deg}}$ in such a way as to obtain the same beamwidth of the reference pattern, and an array with the same number of elements N and the same assigned length L_a has been considered. The pattern synthesized with the presented algorithm exhibited slightly lower maximum sidelobe levels in most of these comparison examples, being equal the beamwidth, the array length, and the number of elements. Moreover, it is also

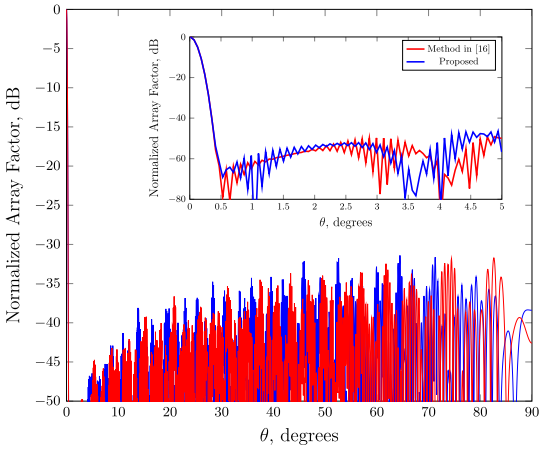

Fig. 1. First example: synthesis of a very narrow beam pattern. Magnification in the window illustrates the pattern behavior for $0° \le \vartheta \le 5°$.

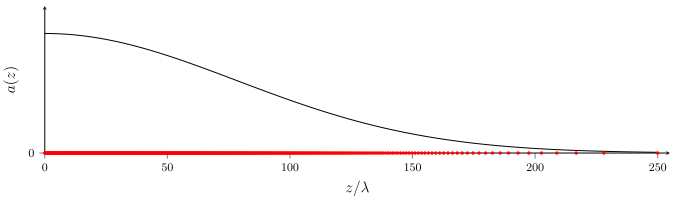

Fig. 2. First example: element positions on the z-axis (red dots) and density distribution $a(z)$, $z \ge 0$ (continuous line).

to be noted that in certain cases (Figs. 4 and 6) the pattern behavior in the entire sidelobe region was considerably improved with the use of the presented algorithm. Another major advantage offered by the proposed algorithm, with respect to the reference ones, is its simplicity, which allows to perform the synthesis essentially in closed form, and in a dramatically low computational time. On the other hand, the developed procedure is suitable for synthesizing only pencil beams and in its present form cannot be used to shape the beam or to control the sidelobe pattern.

Although the proposed method has been developed for the array factor in an ideal environment, an accurate analysis of the mutual coupling effects has been carried out supposing to use half-wave dipoles orthogonal to the z-axis and located at the positions z_n. In each of the considered examples, the simulated radiation pattern in the presence of mutual coupling has some differences with respect to the ideal case. However, such differences are significant only near the mainbeam direction.

A. First Example: Narrow Beam

Consider the synthesis of a linear sparse array with $N = 1001$ elements and length $L_a = 500\lambda$. The standard deviation σ of the desired pattern $F_d(u)$ is chosen in such a way as to obtain a -20 dB beamwidth of 0.5°. Equation (4) with $b = 20$ and $\mathrm{BW}_{\mathrm{deg}} = 0.5$ yields $\sigma = 0.0128$ rad/m. The synthesized array factor is shown in Fig. 1. The element positions and the excitation density $a(z)$ are shown in Fig. 2. Note the typical elements' distribution produced by the density taper approach, with the elements more densely packed where the excitation density is higher, that is, in the central part of the array. The mean distance between adjacent elements is 0.50λ, with minimum value of 0.20λ (for the more central elements) and maximum value of 21.95λ (for the outermost elements). This problem has been solved in 3.6 ms on a laptop with 8 GB of RAM.

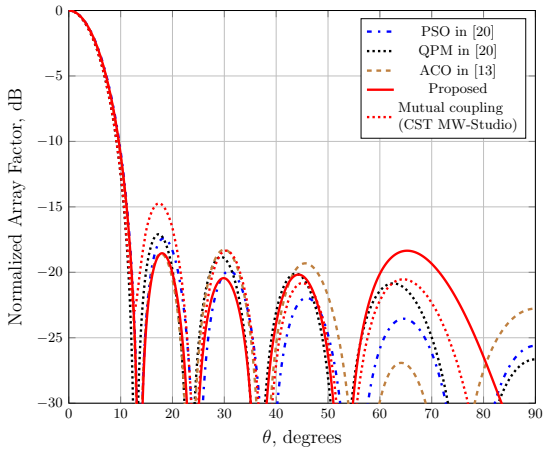

Fig. 3. Second example: synthesized array factor with the proposed Gaussian approach for a 10-element array, in comparison with the results of three previous methods and of the case involving the mutual coupling.

The same narrow beam has also been synthesized by using the method in [16], but using the proposed Gaussian function as the objective array factor mask. This has allowed to solve in [16, eq. (16)] in closed form, instead of using the combined technique proposed in [16], which is based on the Gauss–Kronrod quadrature formula and the Newton–Raphson root-finding method. This has allowed to dramatically reduce the computational burden and the computational time without modifying the results. Fig. 1 shows that, in the two cases, the obtained patterns exhibit essentially the same sidelobe level and beamwidth. The array synthesized with the method in [16] is slightly larger ($L_a = 515.18\lambda$, with mean distance between adjacent elements of 0.51λ, minimum and maximum value of 0.20λ and 25.26λ for the more central elements and for the outermost elements, respectively). The computational time is 39.2 ms on the same laptop, against the 3.6 ms of the presented algorithm. In this regard, it is interesting to note that the method in [16] has been declared to be faster than the global optimization technique developed in [18] and considerably faster than an evolutionary procedure based on the genetic algorithms [19].

B. Comparisons With Examples From Previous Literature

In the following, since the optimal element positions z_n are symmetrically placed with respect to the array center, only the positions with positive abscissas are reported, and are indicated by p_n (the complete set of abscissas z_n is immediately found by symmetry).

1) Second Example: In [20], a particle swarm optimization (PSO) algorithm was used to synthesize a 10-element linear array of length $L_a = 4.3\lambda$, with suppressed sidelobes in the regions $[-90°, -8°]$ and $[8°, 90°]$. The results were compared with those obtained with the quadratic programming method (QPM). The obtained array geometries were given in [20, Table I] and are not reported here. The obtained array factors are shown in Fig. 3 for comparison purposes. The same numerical example was also solved in [13] with an ant colony optimization (ACO) algorithm, obtaining the array factor in Fig. 3 (and the positions listed [13, Table II]). According to the rule introduced at the end of Section II-B, the value of σ has been evaluated by setting in (4) $b = 3$ and $\mathrm{BW}_{\mathrm{deg}} = 7.8$, which is half the desired beamwidth. The following positions (normalized to λ) were obtained: $p_1 = 0.1979$, $p_2 = 0.6023$, $p_3 = 1.0351$, $p_4 = 1.5278$, and $p_5 = 2.1500$ (with minimum and maximum distance between adjacent elements of 0.4044λ and 0.6222λ, respectively). The array factor is shown in Fig. 3 in red. Table I compares the maximum sidelobe levels obtained with the four methods. All the above patterns are ideal array factors. Fig. 3 also shows the radiation pattern (red dotted line) obtained by accurately taking into account the mutual coupling effects, for an array of equally fed half-wave dipoles located at the synthesized positions and orthogonal to the z-axis.

TABLE I

SECOND EXAMPLE: MAXIMUM SIDELOBE LEVELS (IN DECIBELS) OF THE ARRAY FACTORS IN FIG. 3

QPM: -17.09	PSO: -17.40	ACO: -18.27	Proposed: -18.36

TABLE II

THIRD EXAMPLE: SYNTHESIZED ELEMENT POSITIONS (NORMALIZED TO λ) FOR THE 32-ELEMENT ARRAY (PROPOSED METHOD)

$p_1 = 0.2163$	$p_2 = 0.6496$	$p_3 = 1.0853$	$p_4 = 1.5250$
$p_5 = 1.9704$	$p_6 = 2.4235$	$p_7 = 2.8864$	$p_8 = 3.3614$
$p_9 = 3.8515$	$p_{10} = 4.3601$	$p_{11} = 4.8913$	$p_{12} = 5.4505$
$p_{13} = 6.0445$	$p_{14} = 6.6827$	$p_{15} = 7.3781$	$p_{16} = 8.1500$

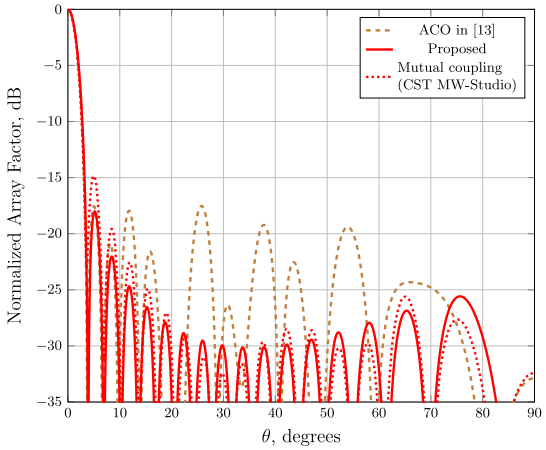

Fig. 4. Third example: comparison of the normalized array factors obtained with the proposed Gaussian approach and with the ACO algorithm in [13], for a 32-element linear array.

2) Third Example: The third example is directly taken from [13], where the ACO algorithm was used to synthesize a 32-element linear array of length $L_a = 16.3\lambda$. The positions obtained by using the proposed method, with $b = 3$ and $\mathrm{BW}_{\mathrm{deg}} = 2.1$, are listed in Table II (and resulted in a minimum and a maximum distance between adjacent elements of 0.4326λ and 0.7719λ, respectively), while those obtained with the ACO algorithm are listed in [13, Table 5]. Both the corresponding array factors are shown in Fig. 4, and exhibit a maximum sidelobe level of -18.10 dB (proposed method) and -17.53 dB (ACO). Thus, in this example, the proposed approach gave a slightly better performance in terms of maximum sidelobe level, but a considerable pattern improvement in the entire sidelobe region.

3) Fourth Example: The fourth example refers to the problem of synthesizing a 31-element array of length $L_a = 9\lambda$. This problem was solved in [21] with a Legendre series expansion, and in [11] using the differential evolution algorithm (DEA). Reference [11, Table 2] lists the element positions obtained with both methods, whereas Table III gives the positions obtained with the approach proposed in this communication, applied setting $b = 3$ and $\mathrm{BW}_{\mathrm{deg}} = 2.08$. The minimum and the maximum distances between adjacent elements were 0.4768λ and 0.9485λ, respectively. Fig. 5 shows the three normalized array

TABLE III

FOURTH EXAMPLE: SYNTHESIZED ELEMENT POSITIONS (NORMALIZED TO λ) FOR THE 31-ELEMENT ARRAY (PROPOSED METHOD)

$p_0 = 0$	$p_1 = 0.4768$	$p_2 = 0.9556$	$p_3 = 1.4387$
$p_4 = 1.9281$	$p_5 = 2.4264$	$p_6 = 2.9364$	$p_7 = 3.4613$
$p_8 = 4.0048$	$p_9 = 4.5717$	$p_{10} = 5.1678$	$p_{11} = 5.8009$
$p_{12} = 6.4814$	$p_{13} = 7.2241$	$p_{14} = 8.0515$	$p_{15} = 9.0000$

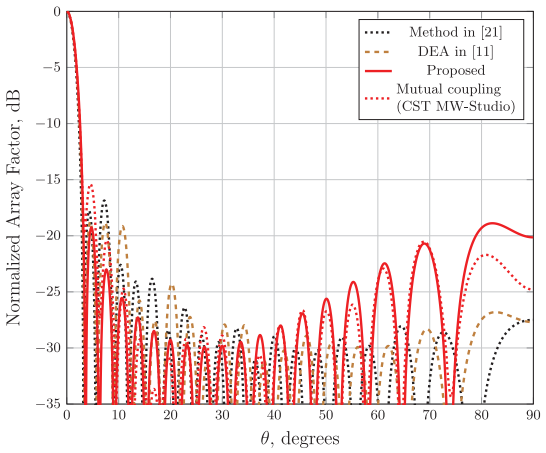

Fig. 5. Fourth example: comparison of the normalized array factors obtained with the proposed Gaussian approach, the algorithm proposed in [21], and the DEA algorithm proposed in [11], for a 31-element linear array.

TABLE IV

FIFTH EXAMPLE: SYNTHESIZED ELEMENT POSITIONS (NORMALIZED TO λ) FOR THE 24-ELEMENT ARRAY (PROPOSED METHOD)

$p_1 = 0.1671$	$p_2 = 0.5025$	$p_3 = 0.8418$	$p_4 = 1.1876$
$p_5 = 1.5430$	$p_6 = 1.9120$	$p_7 = 2.2990$	$p_8 = 2.7105$
$p_9 = 3.1549$	$p_{10} = 3.6451$	$p_{11} = 4.2019$	$p_{12} = 4.8625$

factors. With regard to these patterns, it is interesting to note that, although the maximum sidelobe levels obtained with the Gaussian approach (-18.89 dB) and with the DEA algorithm (-18.75 dB) are similar (a higher value of -16.88 dB was obtained in [21]), the Gaussian approach exhibits its higher sidelobes near the end-fire direction. However, when a suitable element pattern is adopted, the sidelobes near the end-fire direction can be lowered, thus resulting in a substantial improvement of the power pattern synthesized with the proposed method.

4) Fifth Example: The fifth example is taken from [16], where an analytical approach based on the concept of auxiliary array factor was developed. Reference [16, Table 1] lists the element positions obtained for a 24-element uniformly fed aperiodic array of length $L_a = 9.725\lambda$, giving the array factor in Fig. 6, which also shows the normalized array factor obtained with the here proposed Gaussian approach, applied setting $b = 3$ and $\mathrm{BW}_{\mathrm{deg}} = 3.9$. The maximum sidelobe levels were -19.84 dB (method in [16]) and -19.71 dB (proposed method). However, the global behavior of the sidelobe pattern is considerably improved when using the proposed approach. Table IV lists the optimized element positions. The minimum and the maximum distances between adjacent elements were 0.3342λ and 0.6606λ, respectively.

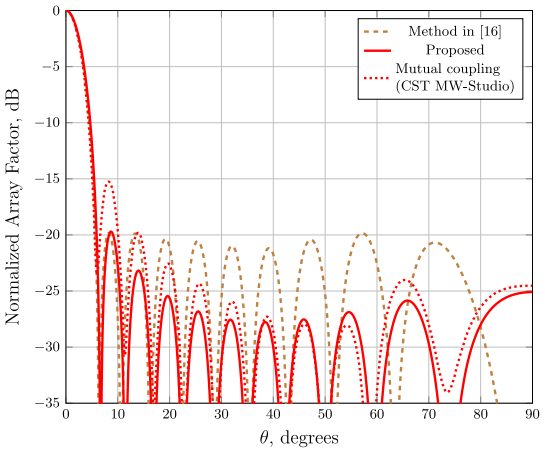

Fig. 6. Fifth example: comparison of the normalized array factors obtained with the proposed Gaussian approach and with the algorithm proposed in [16].

IV. CONCLUSION

In this communication, a fully deterministic method was presented for the synthesis of uniformly fed and nonuniformly spaced linear arrays radiating pencil beams. The proposed synthesis procedure uses a density tapering approach in conjunction with a proper choice of the function representing the desired pencil beam. The main novelty with respect to previous literature is that this function is a Gaussian distribution whose standard deviation is used to control the beamwidth. It is this choice that allows to keep the synthesis procedure extremely simple. As a further advantage, all of the synthesis steps can be implemented in closed form. The only exception is the solution of (16) and (19), which required an iterative technique (we used the bisection method). However, also these equations are solved in real time with extreme accuracy. As a result, the computational times are extremely low (of the order of milliseconds), also when thousands of array elements are involved. Some significant numerical examples showed the improvement that the presented method can provide in comparison with state-of-the art results. As an important remark, it is to be observed that the proposed method yields its best performances for antenna arrays composed by a very great number of elements which radiates very narrow beams, which are typical in satellite applications and are expected to be used in future 5G communication networks. Finally, the results showed that the synthesized patterns provided by the presented method are not strongly affected by the mutual coupling effects.

APPENDIX
DETERMINATION OF L FROM L_a

A. Case of Array Elements in the Barycenters

With the choice (9b), the position z_1 of the first element is given by (13) for $n = 1$. On the other hand, we impose the condition $z_1 = -L_a/2$ (see Section II-A) and $s_0 = -L/2$ (see Section II-B). Substituting the latter two relations into (13) with $n = 1$ yields the following relation between L and L_a:

$$L_a = \frac{2N}{\sigma\sqrt{2\pi}\,\mathrm{erf}\left[\frac{\sigma L}{2\sqrt{2}}\right]}\left[\exp\left(-\frac{\sigma^2 s_1^2}{2}\right) - \exp\left(-\frac{\sigma^2 L^2}{8}\right)\right]. \quad (14)$$

On the other hand, setting $n = 1$ in (12) yields

$$s_1 = -\frac{\sqrt{2}}{\sigma}\,\mathrm{erf}^{-1}\left\{\left(1 - \frac{2}{N}\right)\mathrm{erf}\left[\frac{\sigma L}{2\sqrt{2}}\right]\right\}. \quad (15)$$

Note in (15) that $s_1<0$, as it is assumed that $N>2$. Substituting (15) into (14) yields

$$L_a = \frac{2N}{\sigma\sqrt{2\pi}\,\mathrm{erf}\left[\frac{\sigma L}{2\sqrt{2}}\right]} \cdot \left[\exp\left(-\left\{\mathrm{erf}^{-1}\left[\left(1-\frac{2}{N}\right)\mathrm{erf}\left[\frac{\sigma L}{2\sqrt{2}}\right]\right]\right\}^2\right) - \exp\left(-\frac{\sigma^2 L^2}{8}\right)\right]. \quad (16)$$

Before solving (16) for L, it is necessary to show some helpful properties of it. Precisely, let us denote with $g(L)$ the right-hand side of (16). It can be shown that, for any (positive) σ and N, the function $g(L)$ is increasing and bounded above. In fact, the following can be verified.

1) For any $L > 0$, $g(L)$ yields the length $L_a = -2z_1$, where z_1 is given by (13).
2) z_1 is the abscissa of the barycenter of the region V_1 located between the diagram of $a(z)$ in (5) and the interval $I_1 = [-L/2, s_1]$, where s_1 is given by (15).

By (15), the derivative of s_1 with respect to L is given by

$$\frac{ds_1}{dL} = -\frac{\left(1-\frac{2}{N}\right)\exp\left(-\frac{\sigma^2 L^2}{8}\right)}{2\exp\left\{-\left(\mathrm{erf}^{-1}\left[\left(1-\frac{2}{N}\right)\mathrm{erf}\left(\frac{\sigma L}{2\sqrt{2}}\right)\right]\right)^2\right\}} < 0. \quad (17)$$

Thus, when L increases, the quantity $s_1(<0)$ decreases. So, both extreme points of the integration interval I_1 decrease, that is, they move toward left along the z-axis. As a consequence, the region V_1 moves toward left while remaining below the diagram of $a(z)$. Hence, the abscissa z_1 of the barycenter of V_1 decreases, and therefore the length $L_a = -2z_1$ increases. We can conclude that $g(L)$ is an increasing function. Furthermore, for $L \to +\infty$, $g(L)$ converges to

$$(L_a)_{\sup} = \frac{2N}{\sigma\sqrt{2\pi}}\exp\left\{-\left[\mathrm{erf}^{-1}\left(1-\frac{2}{N}\right)\right]^2\right\} \quad (18)$$

which therefore is the minimum upper bound of $g(L)$. From the above demonstration, the right-hand side of (16) takes all values in the interval $[0, (L_a)_{\sup}[$. As a consequence, given any value of L_a such that $0<L_a<(L_a)_{\sup}$, (16) has a unique solution, which can be accurately evaluated numerically. Many numerical tests showed that, by using the bisection method, the solution L of (16) is found in real time with excellent accuracy.

B. Case of Array Elements in the Middle Points

With the choice (9c), the position of the first element is $z_1 = (-L/2 + s_1)/2$, and since $z_1 = -L_a/2$, it results $s_1 = -L_a + L/2$. Substituting the latter in (12) for $n = 1$, after some manipulations, the following equation is obtained in the unknown L:

$$L = \frac{2\sqrt{2}}{\sigma}\,\mathrm{erf}^{-1}\left\{\frac{N}{2-N}\,\mathrm{erf}\left[\frac{\sigma}{\sqrt{2}}(-L_a + L/2)\right]\right\}. \quad (19)$$

This equation has a unique solution. In fact, since the function $\mathrm{erf}(x)$ assumes all values in the interval $(-1, 1)$, the argument in brace in (19) must belong to such interval, and consequently

$$L_{\min} < L < L_{\max} \quad (20)$$

where

$$L_{\min} = 2L_a - \frac{2\sqrt{2}}{\sigma}\,\mathrm{erf}^{-1}\left(\frac{N-2}{N}\right) \quad (21a)$$

$$L_{\max} = 2L_a + \frac{2\sqrt{2}}{\sigma}\,\mathrm{erf}^{-1}\left(\frac{N-2}{N}\right) \quad (21b)$$

with $N>2$. On the other hand, since the function $\mathrm{erf}(x)$ is increasing, so is its inverse $\mathrm{erf}^{-1}(x)$. But, being $N/(2-N) < 0$, the argument of erf^{-1} in (19) is decreasing, and hence also the right-hand side of (19) is decreasing as a function of L. Moreover, it tends to $+\infty$ when $L \to L^+_{\min}$ and to $-\infty$ when $L \to L^-_{\max}$. Instead, the left-hand side in (19) (L) is trivially increasing. Thus, (19) admits a unique solution. Again, we numerically verified that a possible, very fast, very accurate, and easy way to evaluate such a solution is that of using the bisection method.

REFERENCES

[1] R. L. Haupt and Y. Rahmat-Samii, "Antenna array developments: A perspective on the past, present and future," *IEEE Antennas Propag. Mag.*, vol. 57, no. 1, pp. 86–96, Feb. 2015.

[2] G. Buttazzoni and R. Vescovo, "An efficient and versatile technique for the synthesis of 3D copolar and crosspolar patterns of phase-only reconfigurable conformal arrays with DRR and near-field control," *IEEE Trans. Antennas Propag.*, vol. 62, no. 4, pp. 1640–1651, Apr. 2014.

[3] C. A. Balanis, *Antenna Theory: Analysis and Design*, 2nd ed. New York, NY, USA: Wiley, 2007.

[4] F. J. Ares-Pena, J. A. Rodriguez-Gonzalez, E. Villanueva-Lopez, and S. R. Rengarajan, "Genetic algorithms in the design and optimization of antenna array patterns," *IEEE Trans. Antennas Propag.*, vol. 47, no. 3, pp. 506–510, Mar. 1999.

[5] G. Buttazzoni and R. Vescovo, "Deterministic and stochastic approach to the synthesis of conformal arrays for SAR applications," in *Proc. Int. Conf. Electromagn. Adv. Appl.*, Turin, Italy, Sep. 2013, pp. 520–523.

[6] H. Unz, "Linear arrays with arbitrarily distributed elements," *IRE Trans. Antennas Propag.*, vol. 8, no. 2, pp. 222–223, Mar. 1960.

[7] R. Willey, "Space tapaering of linear and planar arrays," *IRE Trans. Antennas Propag.*, vol. 10, no. 4, pp. 369–377, Jul. 1962.

[8] Y. T. Lo and S. W. Lee, "A study of space-tapered arrays," *IEEE Trans. Antennas Propag.*, vol. AP-14, no. 1, pp. 22–30, Jul. 1966.

[9] G. Buttazzoni and R. Vescovo, "Synthesis of sparse arrays radiating shaped beams," in *Proc. IEEE Antennas Propag. Int. Symp.*, Fajardo, PR, USA, Jun./Jul. 2016, pp. 1–4.

[10] G. Buttazzoni and R. Vescovo, "A deterministic approach to the synthesis of sparse arrays with far-field and near-field constraints," in *Proc. IEEE-APS Antennas Propag. Wireless Commun. Topical Conf.*, Turin, Italy, Sep. 2015, pp. 161–164.

[11] D. G. Kurup, M. Himdi, and A. Rydberg, "Synthesis of uniform amplitude unequally spaced antenna arrays using the differential evolution algorithm," *IEEE Trans. Antennas Propag.*, vol. 51, no. 9, pp. 2210–2217, Sep. 2003.

[12] O. Quevedo-Teruel and E. Rajo-Iglesias, "Ant colony optimization for array synthesis," in *Proc. IEEE Antennas Propag. Int. Symp.*, Albuquerque, NM, USA, Jul. 2006, pp. 3301–3304.

[13] E. Rajo-Iglesias and O. Quevedo-Teruel, "Linear array synthesis using an ant-colony-optimization-based algorithm," *IEEE Antennas Propag. Mag.*, vol. 49, no. 2, pp. 70–79, Apr. 2007.

[14] N. Jin and Y. Rahmat-Samii, "Advances in particle swarm optimization for antenna designs: Real-number, binary, single-objective and multiobjective implementations," *IEEE Trans. Antennas Propag.*, vol. 55, no. 3, pp. 556–567, Mar. 2007.

[15] O. M. Bucci, M. D'Urso, T. Isernia, P. Angeletti, and G. Toso, "Deterministic synthesis of uniform amplitude sparse arrays via new density taper techniques," *IEEE Trans. Antennas Propag.*, vol. 58, no. 6, pp. 1949–1958, Jun. 2010.

[16] D. Caratelli and M. C. Viganò, "A novel deterministic synthesis technique for constrained sparse array design problems," *IEEE Trans. Antennas Propag.*, vol. 59, no. 11, pp. 4085–4093, Nov. 2011.

[17] B. Fuchs, A. Skrivervik, and J. R. Mosig, "Synthesis of uniform amplitude focused beam arrays," *IEEE Antennas Wireless Propag. Lett.*, vol. 11, pp. 1178–1181, Oct. 2012.

[18] W. L. Doyle, "On approximating linear array factors," Rand Corp., Santa Monica, CA, USA, Tech. Memo. RM-3530-PR, Feb. 1963.

[19] R. L. Haupt, "Thinned arrays using genetic algorithms," *IEEE Trans. Antennas Propag.*, vol. 42, no. 7, pp. 993–999, Jul. 1993.

[20] M. M. Khodier and C. G. Christodoulou, "Linear array geometry synthesis with minimum sidelobe level and null control using particle swarm optimization," *IEEE Trans. Antennas Propag.*, vol. 53, no. 8, pp. 2674–2679, Aug. 2005.

[21] B. P. Kumar and G. R. Branner, "Synthesis of unequally spaced linear arrays by Legendre series expansion," in *Proc. IEEE Antennas Propag. Soc. Int. Symp.*, vol. 4. Montreal, QC, Canada, Jul. 1997, pp. 2236–2239.